

See discussions, stats, and author profiles for this publication at: <https://www.researchgate.net/publication/15656098>

# Determination of Stereospecific Assignments, Torsion–Angle Constraints, and Rotamer Populations in Proteins Using the Program Anglesearch

ARTICLE *in* JOURNAL OF MAGNETIC RESONANCE SERIES B · AUGUST 1995

Impact Factor: 2.53 · DOI: 10.1006/jmrb.1995.1099 · Source: PubMed

---

CITATIONS

26

---

READS

31

5 AUTHORS, INCLUDING:



Vladimir Polshakov

Lomonosov Moscow State University

70 PUBLICATIONS 521 CITATIONS

SEE PROFILE



James Feeney

MRC National Institute for Medical Resea...

315 PUBLICATIONS 7,804 CITATIONS

SEE PROFILE

# Determination of Stereospecific Assignments, Torsion-Angle Constraints, and Rotamer Populations in Proteins Using the Program AngleSearch

V. I. POLSHAKOV,\* T. A. FRENKIEL,† B. BIRDSALL,\* A. SOTERIOU,\* AND J. FEENEY\*

\*Laboratory of Molecular Structure, and †MRC Biomedical NMR Centre, National Institute for Medical Research, Mill Hill, London NW7 1AA, United Kingdom

Received September 26, 1994; revised November 18, 1994

A general program, AngleSearch, which calculates coupling constants and interproton distances for any molecular fragment and does a grid search to find torsion angles, rotamer populations, and stereospecific assignments which fit the measured data has been developed. The program takes full advantage of the fact that ratios of cross-peak intensities (measured in HNHB and HN(CO)HB experiments) can provide accurate ratios of coupling constants even for large molecules. AngleSearch is capable of: (a) analyzing any type of residue including protein, RNA, DNA, and ligand residues; (b) conformational grid searching in dihedral-angle space using  $6^\circ$  steps; (c) averaging coupling constants and  $\langle 1/r^6 \rangle$  distances for rotamers undergoing fast exchange; (d) grid or Monte Carlo searching for populations of staggered rotamers; (e) using all available distance-related data from ROESY and/or NOESY spectra; (f) using any available coupling constant data having known relationships to corresponding dihedral angles; and (g) directly using cross-peak intensities related to values of coupling constants. The program can also assist in the stereospecific assignment of the  $\alpha$ -CH<sub>2</sub> protons of glycine residues. The effects of the quality of the input data on the results of the AngleSearch calculations have been assessed. © 1995 Academic Press, Inc.

## INTRODUCTION

Nuclear magnetic-resonance measurements are now being used routinely to determine three-dimensional structures of proteins in solution. This involves first making specific assignments for the NMR signals of all the protein protons and then measuring interproton NOEs to provide distance constraints to be used in distance geometry or simulated annealing calculations (1). In order to obtain high-quality structures from these calculations, it is also necessary to include torsion-angle constraints and data from stereospecifically assigned pairs of prochiral protons and methyl groups in the protein (2–7). If stereospecific assignments are not available, then one must resort to replacing each pair of unassigned methylene protons or methyl groups with a pseudatom when describing NOE-based distance constraints; this leads to lower-quality structures because of the less specific distance constraints introduced into the calculations. An ad-

ditional benefit results from making stereospecific assignments in that these often allow a more precise definition of the local conformation around adjacent torsion angles which in turn contributes to higher-quality structures.

Methods of making stereospecific assignments based on using conformationally sensitive spin-coupling constant and NOE data have been developed (8). Some of these methods were originally used to obtain such information for amino acids and small peptides (9, 10) and, more recently, have been extended to studies of proteins (3–8, 11, 12). Other workers (13) have developed a program (CUPID) for calculating rotamer probability distributions from NMR coupling constant and NOE data.

Programs have been reported for systematically calculating NMR data for sets of torsion angles and then finding ranges of torsion angles consistent with experimentally observed data (12, 14, 15). These programs proved useful when only limited data were available. Recent advances in methodology allow a larger number of conformationally related parameters to be measured, particularly those involving heteronuclear coupling constants, where fairly precise values can now be estimated even in NMR spectra of proteins. In some experiments, the coupling constants can be obtained by direct measurement of splittings in the resolved multiplets (16–18). In other experiments (such as HNHA, HNHB, HN(CO)HB, and TOCSY-based experiments), the intensities of cross peaks can be related to the coupling constants (19–22).

We have developed a conformational search program (AngleSearch) which takes advantage of the increased information now available and also explicitly deals with the important case where there is rotameric averaging of the parameters. The program is general in that it can be used to examine not only proteins but also DNA, RNA, and other biopolymers. It is not restricted to particular residues (for example, it can deal with prolines and glycines) or sets of torsion angles and can be used to assist in assigning any pair of prochiral protons in a molecule, including the  $\alpha$ -protons in glycine residues. Using the program, we have been able to make stereospecific assignments for many pairs of protons

and methyl groups for several proteins (including various complexes of *Lactobacillus casei* DHFR) and also to obtain detailed local conformational information for use in structural calculations.

### OUTLINE OF THE AngleSearch PROGRAM

AngleSearch is a general program which calculates coupling constants and interproton distances for each torsion angle and for pairs of adjacent torsion angles in any biopolymer (for example, a protein) and does a grid search to find which torsion angles and stereospecific assignments are consistent with the measured coupling constants and interproton distances or the intensity data related to them. The torsion angles in larger fragments of the molecule are explored by considering results from combinations of these one- and two-torsion-angle fragments. For residues where the data are inconsistent with a single conformation, solutions can be obtained based on averaging  $\langle J \rangle$  and  $\langle r^{-6} \rangle$  in mixtures of conformers.

Although AngleSearch is a general program, here we consider its application to conformational studies of proteins where the structure can be defined in terms of the variable torsion angles  $\phi$ ,  $\psi$ , and  $\chi$ . Tables 1 and 2 show the various three-bond coupling constants and interproton distances,

together with their corresponding related dihedral angles. Also included in Tables 1 and 2 are the various NMR experiments which can be used to provide data related to the spin-coupling constants and interproton distances.

### Coupling Constants

AngleSearch systematically calculates three-bond ( $^3J$ ) coupling constants for various values of dihedral angles  $\theta$  by using generalized Karplus equations of the type

$$^3J = A \cos^2 \theta + B \cos \theta + C \quad [1]$$

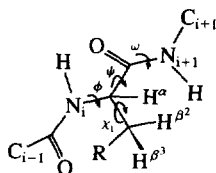
with

$$\theta = \text{torsion angle } (\phi, \psi, \text{ etc.}) + \zeta,$$

where  $A$ ,  $B$ , and  $C$  are constants for particular fragments in different residues and  $\zeta$  are phase shifts depending on the specific pair of nuclei involved in the spin-coupling interactions (see Table 3). Each calculated curve can be displayed graphically and this feature is useful when the phase shifts are being introduced.

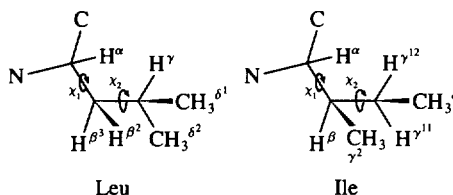
Using a grid search, NMR-determined coupling constants are compared with values calculated from the Karplus equation [1]. Heteronuclear coupling constants are also included in the calculations. In favorable cases where a torsion angle

TABLE 1  
Experiments Used to Determine Interproton Distances and Spin-Coupling Constants Required for Determination of  $\phi$ ,  $\psi$ , and  $\chi$ , Torsion Angles in Proteins



Coupling constants	Angle	Experiments	References
$^3J(\text{HN}, \text{H}\alpha)$	$\phi$	HNHA, DQF-COSY	(20, 25)
$^3J(\text{H}\alpha, \text{H}\beta^{\text{'s}})$	$\chi_1$	TOCSY-HSQC, PE-COSY	(18, 26, 34)
$^3J(^{15}\text{N}, \text{H}\beta^{\text{'s}})$	$\chi_1$	HNHB	(21)
$^3J(^{15}\text{N}, \text{H}\alpha^{i-1})$	$\psi$	HNHB, HMBC	(21, 27)
$^3J(^{13}\text{CO}, \text{H}\beta^{\text{'s}})$	$\chi_1$	HN(CO)HB	(22, 30)
$^3J(^{13}\text{CO}, \text{H}\alpha^{i+1})$	$\phi$	HN(CO)HB	(22)
$^3J(^{13}\text{CO}, \text{HN}^{i-1})$	$\phi$	HNCA, E.COSY	(28)
$^3J(^{13}\text{CH}_3\gamma, \text{H}\alpha)$	$\chi_1$	LRCH	(29)
Distances	Angle(s)	Experiments	References
$d(\text{HN}, \text{H}\alpha)$	$\phi$	2D ROESY, 3D $^{15}\text{N}$ ROESY-HMQC	(23, 24)
$d(\text{HN}, \text{H}\beta^{\text{'s}})$	$\phi, \chi_1$	2D ROESY, 3D $^{15}\text{N}$ ROESY-HMQC	(23, 24)
$d(\text{H}\alpha, \text{H}\beta^{\text{'s}})$	$\chi_1$	2D ROESY, 3D $^{13}\text{C}$ ROESY-HMQC	(19, 23)
$d(\text{HN}^{i+1}, \text{H}\alpha)$	$\psi, (\omega)$	2D ROESY, 3D $^{15}\text{N}$ ROESY-HMQC	(23, 24)
$d(\text{HN}^{i+1}, \text{H}\beta^{\text{'s}})$	$\psi, \chi_1, (\omega)$	2D ROESY, 3D $^{15}\text{N}$ ROESY-HMQC	(23, 24)
$d(\text{H}\delta^{\text{'s}i+1}, \text{H}\alpha)$	$\psi, \chi_1, (\omega)$	2D ROESY, 3D $^{13}\text{C}$ ROESY-HMQC	(19, 23)
$d(\text{H}\delta^{\text{'s}i+1}, \text{H}\beta^{\text{'s}})$	$\psi, \chi_1, (\omega)$	2D ROESY, 3D $^{13}\text{C}$ ROESY-HMQC	(19, 23)

TABLE 2  
Experiments Used to Determine Spin-Spin Coupling Constants and Interproton Distances Required for Determination of  $\chi_2$  Torsion Angles



Residue	Coupling constants	Experiments	Reference
Leu	$^3J(\text{H}\beta^2, \text{H}\gamma), ^3J(\text{H}\beta^3, \text{H}\gamma)$ $^3J(^{13}\text{C}\delta^1, \text{H}\beta^2), ^3J(^{13}\text{C}\delta^1, \text{H}\beta^3)$ $^3J(^{13}\text{C}\delta^2, \text{H}\beta^2), ^3J(^{13}\text{C}\delta^2, \text{H}\beta^3)$ $^3J(^{13}\text{C}\delta^1, ^{13}\text{C}\alpha), ^3J(^{13}\text{C}\delta^1, ^{13}\text{C}\alpha)$	$^{13}\text{C}$ -TOCSY-HMQC $^{13}\text{C}$ - $^1\text{H}$ LRCH $^{13}\text{C}$ - $^1\text{H}$ LRCH $^{13}\text{C}$ - $^{13}\text{C}$ LRCH	(31) (32) (32) (33)
Ile	$^3J(\text{H}\beta, \text{H}\gamma^{11}), ^3J(\text{H}\beta, \text{H}\gamma^{12})$ $^3J(^{13}\text{C}\gamma^2, \text{H}\gamma^{11}), ^3J(^{13}\text{C}\gamma^2, \text{H}\gamma^{12})$ $^3J(^{13}\text{C}\delta, \text{H}\beta)$ $^3J(^{13}\text{C}\delta, ^{13}\text{C}\gamma^2)$	$^{13}\text{C}$ -TOCSY-HMQC $^{13}\text{C}$ - $^1\text{H}$ LRCH $^{13}\text{C}$ - $^1\text{H}$ LRCH $^{13}\text{C}$ - $^{13}\text{C}$ LRCH	(31) (32) (32) (33)
Residue	Distances	Experiments	Reference
Leu	$d(\text{H}\delta^1, \text{H}\beta^2), d(\text{H}\delta^1, \text{H}\beta^3)$ $d(\text{H}\delta^2, \text{H}\beta^2), d(\text{H}\delta^2, \text{H}\beta^3)$ $d(\text{H}\delta^1, \text{H}\alpha), d(\text{H}\delta^2, \text{H}\alpha)$	ROESY, $^{13}\text{C}$ -ROESY-HMQC ROESY, $^{13}\text{C}$ -ROESY-HMQC ROESY, $^{13}\text{C}$ -ROESY-HMQC	(19, 23) (19, 23) (19, 23)
Ile	$d(\text{H}\gamma^{11}, \text{H}\gamma^2), d(\text{H}\gamma^{12}, \text{H}\gamma^2)$ $d(\text{H}\gamma^{11}, \text{H}\alpha), d(\text{H}\gamma^{12}, \text{H}\alpha)$ $d(\text{H}\delta, \text{H}\alpha), d(\text{H}\delta, \text{H}\beta)$	ROESY, $^{13}\text{C}$ -ROESY-HMQC ROESY, $^{13}\text{C}$ -ROESY-HMQC ROESY, $^{13}\text{C}$ -ROESY-HMQC	(19, 23) (19, 23) (19, 23)

can be described by more than one three-bond coupling constant, an unambiguous determination of the angle can usually be made.

In order to take account of local mobility, the program also has the option of calculating locally averaged coupling constants as proposed by Karimi-Nejad *et al.* (39). For this, the torsion angle is assumed to have a Gaussian distribution around a mean value  $\langle\theta\rangle$  with standard deviation  $\sigma$ , and a locally averaged coupling constant  $J_{av}$  is calculated using

$$J_{av} = \frac{1}{\sigma\sqrt{2\pi}} \int_{-\pi}^{\pi} J(\theta) \exp\left[-\frac{(\theta - \langle\theta\rangle)^2}{2\sigma^2}\right] d\theta, \quad [2]$$

where  $J(\theta)$  is calculated from Eq. [1].

The experimentally determined coupling constant information can be obtained either directly from measuring peak positions in multiplets (such as those observed in E.COSY or heteronuclear versions of E.COSY) (8, 17, 18, 39, 40) or indirectly from measuring peak intensities in TOCSY, HNHA, HNHB, or HN(CO)HB experiments (19–22, 34). The indirect methods are particularly useful for large proteins (>10 kDa) where it is difficult to obtain precise values of coupling constants directly from the multiplets. For HNHB or HN(CO)HB experiments in cases where two coupling constants involve a common nucleus (for example,  $^3J_{^{15}\text{N}\beta^2}$  and  $^3J_{^{15}\text{N}\beta^3}$ ) the relative intensities of the cross peaks provide a sensitive measure of the relative values of the two coupling constants, even though precise values of the coupling constants cannot be measured. For example, in the HNHB experiment, the intensity  $I_{\text{NX}}$  of the cross peak is related to the  $J_{\text{NX}}$  coupling constant by the expression (21)

$$I_{\text{NX}} \propto \sin^2(\pi J_{\text{NX}} \Delta) \prod_{\text{K} \neq \text{X}} \cos^2(\pi J_{\text{NK}} \Delta), \quad [3]$$

TABLE 3

Parameters Used in Karplus-Type Equations (See Eq. [1])

Coupling constant	Torsion angle	$\zeta$	A	B	C	Ref.
$^3J(\text{HN}, \text{H}\alpha)$	$\phi$	$-60^\circ$	6.51	-1.76	1.60	(20)
$^3J(\text{HN}, \text{C}\gamma)$	$\phi$	$-180^\circ$	5.7	-2.7	0.1	(35)
$^3J(\text{HN}, \text{C}\beta)$	$\phi$	$+60^\circ$	4.5	-1.5	-0.2	(35)
$^3J(\text{H}\alpha, \text{H}\beta^2)$	$\chi_1$	$-120^\circ$	9.5	-1.6	1.8	(36)
$^3J(\text{H}\alpha, \text{H}\beta^3)$	$\chi_1$	$0^\circ$	9.5	-1.6	1.8	(36)
$^3J(\text{N}, \text{H}\beta^2)$	$\chi_1$	$120^\circ$	-4.4	1.2	0.1	(37)
$^3J(\text{N}, \text{H}\beta^3)$	$\chi_1$	$-120^\circ$	-4.4	1.2	0.1	(37)
$^3J(\text{C}^1, \text{H}\beta^2)$	$\chi_1$	$0^\circ$	7.20	-2.04	0.6	(38)
$^3J(\text{C}^1, \text{H}\beta^3)$	$\chi_1$	$120^\circ$	7.20	-2.04	0.6	(38)

where  $\Delta$  is the HMQC delay in the HNHB pulse sequence and K refers to protons other than X. In our case, the ratio of intensities  $I_{N\beta^2}/I_{N\beta^3}$  from Eq. [3] is given by

$$\frac{I_{N\beta^2}}{I_{N\beta^3}} = \frac{\tan^2(\pi J_{N\beta^2} \Delta)}{\tan^2(\pi J_{N\beta^3} \Delta)} \quad [4]$$

Figure 1 illustrates the dependence of the logarithm of the ratio of such intensities (measured in HNHB experiments) on the  $\chi_1$  torsion angle, where  $J_{N\beta^2}$  and  $J_{N\beta^3}$  have been calculated using Eq. [2] with  $\sigma = 15.0^\circ$ . Because the intensity ratio is a strong function of  $\chi_1$ , it provides valuable additional constraints on the torsion angles and assists in the determination of stereospecific assignments.

Although three-bond coupling constants are those most easily correlated with dihedral angles, there are several examples of other couplings (41–43) which show dihedral-angle dependence on one or two angles. Such data can be incorporated into AngleSearch once the conformational dependence is known.

#### Interproton Distances

AngleSearch also systematically calculates interproton distances as a function of dihedral angles by using explicit trigonometric expressions which relate the distances to appropriate bond lengths, covalent bond angles, and dihedral angles for molecular fragments in any type of residue. These calculated distances are compared with ranges of NMR-determined estimates from NOESY- and ROESY-type experiments (see Tables 1 and 2). The ROESY experiments are preferable because ROESY cross-peak intensities are less affected by spin diffusion than are NOESY cross peaks at analogous mixing times (19, 44). In cases where one proton is near to two others (for example, an  $\alpha$ -CH near to  $\beta$ -CH<sub>2</sub> protons), ratios of intensities can be usefully interpreted in terms of distance ratios and this allows the program to be more discriminating in the search for acceptable torsion angles and stereospecific assignments consistent with the data.

For small proteins (<10 kDa), 2D ROESY experiments can usually supply enough distance information for AngleSearch to yield  $\psi$ ,  $\phi$ ,  $\chi_1$ , and  $\chi_2$  torsion-angle constraints and stereospecific assignments. For larger proteins, such as DHFR (18.3 kDa), it is necessary to use 3D ROESY-HMQC experiments to obtain such information. Three-dimensional <sup>15</sup>N ROESY-HMQC measurements are adequate for defining  $\psi$ ,  $\phi$ , and  $\chi_1$  torsional-angle constraints and  $\beta$ -CH<sub>2</sub> stereospecific assignments but 3D <sup>13</sup>C ROESY-HMQC experiments are necessary if one requires distance information to characterize the  $\chi_2$  torsion angle. The latter <sup>13</sup>C-based experiment is also required to provide the necessary distance information for determining  $\psi$  and  $\chi_1$  angles for residues which precede proline.

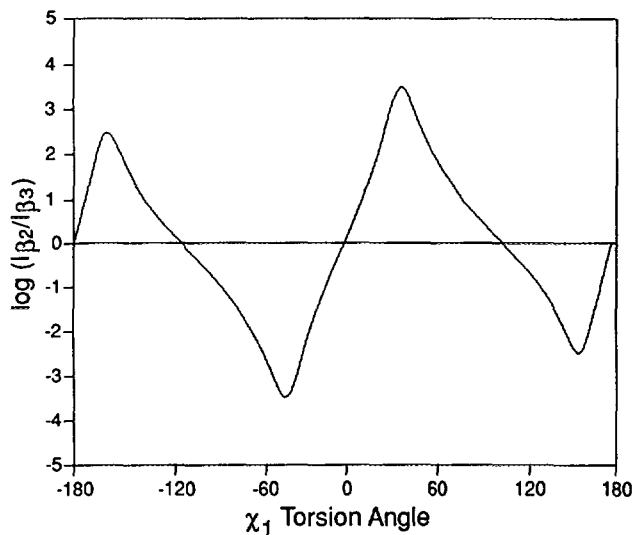


FIG. 1. Plot of  $(I_{N\beta^2}/I_{N\beta^3})$  versus  $\chi_1$  torsion angle, where  $I_{N\beta^2}$  and  $I_{N\beta^3}$  are the intensities of the cross peaks in the HNHB spectrum corresponding to the <sup>15</sup>N-H $\beta^2$  and <sup>15</sup>N-H $\beta^3$  coupling constants.

#### Calculation Procedures

Two main approaches for analyzing the data are used in the program:

**Single conformation.** In this case, the program assumes a single conformation and calculates the coupling constants and interproton distances for each torsion angle or pair of adjacent torsion angles and uses a grid search in 6° steps to find which torsion angles are consistent with the measured data.

**Conformational averaging.** In this case, the program assumes the presence of rotational isomers undergoing fast exchange averaging and fits the observed data to calculated data from mixtures of rotamers. For example, for a set of  $\phi$ ,  $\psi$ , and  $\chi_1$  torsion angles, a grid search for  $\phi$  and  $\psi$  angles is combined with a grid or Monte Carlo search for the rotamer populations for  $\chi_1$ . Again, if sufficient high-quality input data are available, this results in  $\phi$  and  $\psi$  angles,  $\chi_1$  rotamer populations, and stereospecific assignments which fit the data. This approach will find all the solutions obtained using the single-conformation approach (except those which have nonstaggered  $\chi_1$  angles) and additionally will find solutions where averaging of side-chain rotamers is taking place. In cases where there is either less information or lower-quality information available, the determined angle constraints cover a wider range of conformational space and sometimes the stereospecific assignments cannot be made without resorting to other methods (see Tables 4 and 5).

The conformational averaging about the  $\chi_1$  torsion angle assumes the presence of a mixture of the three staggered rotameric states ( $\chi_1 = 180^\circ, -60^\circ, 60^\circ$ ) rapidly interconverting on the chemical-shift time scale such that only a

**TABLE 4**  
**Accuracy of Calculated Torsion Angles and Stereospecific Assignment Determination Obtained Using Input Data**  
**of Varying Quality Related to  $\alpha$ -Helical and  $\beta$ -Strand Residues**

Initial set of angles			Data set	Coupling constants (Hz)					ROESY effects <sup>b</sup>	Stereospecific assignment	Results		
$\chi_1$	$\phi$	$\psi$		$^3J_{NH,H\alpha}$	$^3J_{H\alpha,H\beta}$	$^3J_{H\alpha,H\beta'}$	$^3J^{15}N,H\beta$	$^3J^{15}N,H\beta'$			$\chi_1$	$\phi$	$\psi$
α-Helices													
−60° <sup>a</sup>	−60°	−50°	A	4.1 ± 0.25	12.9 ± 0.25	3.4 ± 0.25	—	—	(1)	Yes	−60° ± 3°	−60° ± 3°	−50° ± 10°
−60°	−60°	−50°	B	4.1 ± 1.0	12.9 ± 1.0	3.4 ± 1.0	—	—	(1)	Yes	−60° ± 6°	−60° ± 10°	−50° ± 6°
−60°	−60°	−50°	C	<6.0	>6.0	<7.0	—	—	(1)	Yes	−70° ± 20°	−65° ± 15°	−57° ± 20°
−60°	−60°	−50°	D	<6.0	>6.0	<7.0	—	—	(2)	No	−60° ± 25° 185° ± 25°	Undefined	0° ± 90°
−60°	−60°	−50°	E	<6.0	>6.0	<7.0	<3.0	>3.0	(1)	Yes	−65° ± 30°	−50 ± 25	−65° ± 25°
−60°	−60°	−50°	F	<6.0	>6.0	<7.0	<3.0	>3.0	(2)	Yes	−65° ± 30°	Undefined	−65° ± 60°
β-Strands													
−60° <sup>a</sup>	−120°	120°	A	9.9 ± 0.25	12.9 ± 0.25	3.4 ± 0.25	—	—	(1)	Yes	−60° ± 3°	−120° ± 10°	145° ± 25°
−60°	−120°	120°	B	9.9 ± 1.0	12.9 ± 1.0	3.4 ± 1.0	—	—	(1)	Yes	−60° ± 10°	−120° ± 15°	145° ± 25°
−60°	−120°	120°	C	>6.0	>6.0	<7.0	—	—	(1)	No	−60° ± 30° 160° ± 10°	−120° ± 20°	145° ± 25°
−60°	−120°	120°	D	>6.0	>6.0	<7.0	—	—	(2)	No	−65° ± 35° 185° ± 35°	−120° ± 40° 60° ± 20°	120° ± 65°
−60°	−120°	120°	E	>6.0	>6.0	<7.0	<3.0	>3.0	(1)	Yes	−65° ± 30°	−120° ± 20°	145° ± 25°
−60°	−120°	120°	F	>6.0	>6.0	<7.0	<3.0	>3.0	(2)	Yes	−65° ± 30° 60° ± 20°	−120° ± 20°	120° ± 60°

<sup>a</sup> The calculations were also carried out for  $\chi_1$  angles  $180^\circ$  and  $60^\circ$ ; similar results were obtained.

<sup>b</sup> (1) Full set of ROESY effects between all pairs of atoms (HN, H $\alpha$ , H $\beta$ , H $\beta'$ , and HN<sup>i+1</sup>) except H $\alpha$ -H $\beta$  and H $\alpha$ -H $\beta'$ . (2) ROESY effects for only HN-HN<sup>i+1</sup>, HN-H $\alpha$ , and H $\alpha$ -HN<sup>i+1</sup>.

TABLE 5  
Accuracy of Calculated Torsion Angles, Stereospecific Assignments, and Rotamer Populations Determined Using Input Data of Varying Quality Related to  $\alpha$ -Helical and  $\beta$ -Strand Residues

Initial set of angles		Data set <sup>a</sup>	Coupling constants (Hz)							Compare intensities	Stereospecific assignment	Results			
$\phi$	$\psi$		$^3J_{H\alpha,H\beta}$	$^3J_{H\alpha,H\beta'}$	$^3J_{^{15}N,H\beta}$	$^3J_{^{15}N,H\beta'}$	$^3J_{^{13}C,H\beta}$	$^3J_{^{13}C,H\beta'}$	$\phi$			$\psi$	$p_{180^\circ}$	$p_{-60^\circ}$	$p_{+60^\circ}$
$\alpha$ -Helices															
-60°	-50°	A	9.1 ± 0.25	5.75 ± 0.25	1.2 ± 0.25	3.5 ± 0.25	3.6 ± 0.25	3.0 ± 0.25	No	Yes	-60° ± 6°	-50° ± 6°	0.25 ± 0.04	0.60 ± 0.02	0.15 ± 0.04
-60°	-50°	B	9.1 ± 1.0	5.75 ± 1.0	1.2 ± 1.0	3.5 ± 1.0	3.6 ± 1.0	3.0 ± 1.0	No	Yes	-60° ± 6°	-50° ± 6°	0.25 ± 0.10	0.60 ± 0.10	0.15 ± 0.15
-60°	-50°	B	9.1 ± 1.0	5.75 ± 1.0	1.2 ± 1.0	3.5 ± 1.0	—	—	No	Yes	-60° ± 6°	-50° ± 6°	0.27 ± 0.15	0.64 ± 0.15	0.10 ± 0.15
-60°	-50°	C	>7	3-9	<2	>3	—	—	No	Yes <sup>b</sup>	-60° ± 12°	-50° ± 6°	0.24 ± 0.20	0.67 ± 0.20	0.09 ± 0.15
-60°	-50°	C	>7	3-9	<2	>3	—	—	Yes	Yes	-60° ± 12°	-50° ± 6°	0.22 ± 0.12	0.62 ± 0.08	0.16 ± 0.04
$\beta$ -Strands															
-120°	120°	A	9.1 ± 0.25	5.75 ± 0.25	1.2 ± 0.25	3.5 ± 0.25	3.6 ± 0.25	3.0 ± 0.25	No	Yes	120° ± 20°	140° ± 25°	0.25 ± 0.04	0.60 ± 0.02	0.15 ± 0.04
-120°	120°	B	9.1 ± 1.0	5.75 ± 1.0	1.2 ± 1.0	3.5 ± 1.0	3.6 ± 1.0	3.0 ± 1.0	No	Yes	120° ± 20°	120° ± 60°	0.25 ± 0.10	0.60 ± 0.10	0.15 ± 0.15
-120°	120°	B	9.1 ± 1.0	5.75 ± 1.0	1.2 ± 1.0	3.5 ± 1.0	—	—	No	Yes	120° ± 20°	120° ± 60°	0.27 ± 0.15	0.59 ± 0.15	0.14 ± 0.15
-120°	120°	C	>7	3-9	<2	>3	—	—	No	Yes <sup>b</sup>	120° ± 20°	120° ± 60°	0.20 ± 0.20	0.68 ± 0.20	0.13 ± 0.15
-120°	120°	C	>7	3-9	<2	>3	—	—	Yes	Yes	120° ± 20°	120° ± 60°	0.20 ± 0.12	0.65 ± 0.10	0.15 ± 0.05

<sup>a</sup> Set of data includes in all cases ROESY effects between all pairs of atoms (except  $H\alpha-H\beta$  and  $H\alpha-H\beta'$ ) and coupling constants  $^3J(HN,H\alpha)$  measured with accuracy of 1 Hz.

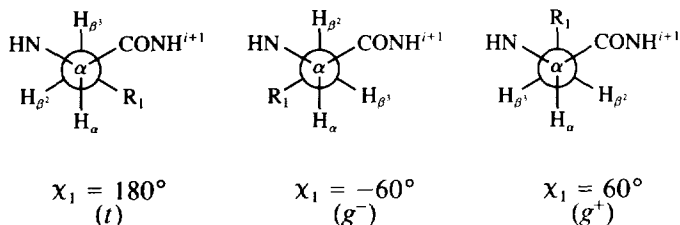
<sup>b</sup> Stereospecific assignments can only be obtained when a full set of interatomic distances is available.

single averaged spectrum is detected. If the fractional populations are defined as  $p_i$  ( $p_{180^\circ}$ ,  $p_{-60^\circ}$ , and  $p_{60^\circ}$ ), then the averaged values of the coupling constants and distance parameters are given by

$$\langle J \rangle = \sum_i p_i \times J_i \quad [5]$$

$$\left\langle \frac{1}{r^6} \right\rangle = \sum_i p_i \times r_i^{-6}, \quad [6]$$

where  $J_i$  and  $r_i$  are the coupling constants and internuclear distances in the individual rotamers:



In the  $6^\circ$  grid search for  $\phi$  and  $\psi$ , the fractional population related to  $x_1$  are also searched in selected steps (0.02 to 0.2). In the Monte Carlo calculations, no limit is placed on the fractional populations increments. In the case where sufficient high-quality data are available, the program finds well-defined solutions for  $x_1$  fractional populations for a narrow range of  $\phi$  and  $\psi$  values. For lower-quality data, a range of fractional populations can fit the data and in these cases the mean values of the populations and their deviations are calculated (see Table 5).

AngleSearch has been developed for an IBM compatible PC and operates under MS-DOS in a fully interactive mode. Using an Intel 486 DX-33 processor, a simple grid search for  $\phi$ ,  $\psi$ , and  $x_1$  typically takes 20–80 s per residue. The final output can be presented in a form which is suitable for inputting into the standard packages available for structure determinations: appropriate outputs for the distance geometry program DIANA or for the molecular dynamics programs X-PLOR and DISCOVER can be selected. The program is available upon request from the authors.

## MATERIALS AND EXPERIMENTAL METHODS

The preparation and purification of uniformly  $^{15}\text{N}$ - and  $^{13}\text{C}$ -labeled *L. casei* DHFR (99% labeled) samples and their complexes have been described previously (45–48).

The NMR experiments were carried out at 308 K using a Varian Unity 600 spectrometer. The experiments used to provide coupling constant information were DQF-COSY (25), HNHA (20), constant-time HNHB (21), and 3D  $^{15}\text{N}$  TOCSY-HMQC (26). The spectra were processed with software written in-house (C. J. Bauer, unpublished), using lin-

ear prediction (49) and zero filling in the indirect dimensions, and zero filling alone in the real-time dimension. The digital resolution in the final data matrices was typically 15.6 Hz/point in the  $^{15}\text{N}$  dimension, and 15.6 and 7.8 Hz/point in the indirect and direct  $^1\text{H}$  dimensions, respectively. In the HNHA and HNHB experiments, the delays which determine the cross-peak intensities were set to the values proposed in the original publications (20, 21). The mixing time employed for the 3D  $^{15}\text{N}$  TOCSY-HMQC was 37 ms. In the HNHA spectra, diagonal and cross peaks were integrated in the  $^1\text{H}$ - $^1\text{H}$  slice of maximum intensity. The values of coupling constants were then calculated from the intensities by using the expression (20)

$$\frac{I_{\text{cross}}}{I_{\text{diag}}} = \tan^2(\pi J \Delta), \quad [7]$$

where  $\Delta$ , the homonuclear dephasing/rephasing delay, was 13.05 ms. Calculated values of  $^3J_{\text{HN,H}\alpha}$  coupling constants were increased by 15% to compensate for the effects of  $^1\text{H}\alpha$  relaxation (20).

Similarly, intensity measurements were made in the HNHB spectra but in this case, it is only possible to deduce the ratio of the coupling constants as discussed earlier. In the spectra obtained from the 3D  $^{15}\text{N}$  TOCSY-HMQC experiments, the relative intensities of the cross peaks were used to indicate the larger and smaller  $J_{\alpha\beta}$  values and it was possible to classify the values as being small (2–7 Hz), medium (4–9 Hz), or large (6–13 Hz) before inputting them into the AngleSearch program.

The experiments used for obtaining interproton distance information included 2D ROESY (23), 3D  $^{15}\text{N}$  ROESY-HMQC (24), and 3D  $^{13}\text{C}$  ROESY-HMQC (19) with mixing times in the range 25–40 ms. The 3D  $^{15}\text{N}$  ROESY-HMQC spectrum was acquired and processed as above; the  $^1\text{H}$  dimensions of the  $^{13}\text{C}$  ROESY-HMQC spectrum was similar but the  $^{13}\text{C}$  dimension had a 5 ms acquisition time and was processed to give a digital resolution of 38 Hz/point. Intensities in these spectra were calibrated by reference to  $\text{H}\alpha^{(i)}-\text{HN}^{(i+1)}$  cross peaks arising from residues in  $\beta$ -strands; other interproton distances were then estimated by classifying the intensities of the cross peaks as very small (1.8–4.5 Å), small (1.8–3.5 Å), medium (1.8–3.2 Å), large (1.8–2.8 Å), or very large (1.8–2.5 Å). A pseudo-atom correction (1 Å) was added to distances obtained from NOEs involving methyl groups.

## VERIFICATION OF THE METHOD

### *Effects of the Quality of the Input Data on the Results of the AngleSearch Calculations*

*Case of fixed conformation.* In order to explore the relationship between the quality of the input data and the re-



sults obtained, we have used AngleSearch to calculate the values of  $\phi$ ,  $\psi$ , and  $\chi_1$  and the stereospecific assignments for various sets of synthetic input data of different qualities and typical of  $\alpha$ -helical and  $\beta$ -strand conformations. The different sets of data include coupling constants of varying accuracy, reflecting data obtained from particular types of experiments, e.g., E.COSY, DQF-COSY (Data Set B in Table 4), and TOCSY contour levels (Data Sets C, D, E, and F), and also containing either complete or incomplete sets of distance-related ROESY data. Consideration of the results from these model calculations allows us to assess the quality of the input data required to achieve certain results.

If the data are very well defined (Data Set A—unlikely to be achievable for proteins), then it is possible to obtain precise results even with limited coupling constant data ( $^3J_{\text{HN,H}\alpha}$ ,  $^3J_{\text{H}\alpha,\text{H}\beta}$  and  $^3J_{\text{H}\alpha,\text{H}\beta'}$ ), providing that a full set of ROESY distance information is also available. In cases where all the three-bond coupling constants ( $^3J_{\text{HN,H}\alpha}$ ,  $^3J_{\text{H}\alpha,\text{H}\beta}$ ,  $^3J_{\text{H}\alpha,\text{H}\beta'}$ ,  $^3J_{\text{HN,H}\beta}$ , and  $^3J_{\text{HN,H}\beta'}$ ) and interproton distances ( $\text{NH}^{(i)}-\text{NH}^{(i+1)}$ ,  $\text{NH}^{(i)}-\text{H}\alpha^{(i)}$  and  $\text{H}\alpha^{(i)}-\text{NH}^{(i+1)}$ ) are available (Data Set F), it is seen that, even with relatively poor data, the stereospecific assignments and estimates of the torsion angles can be obtained. If the coupling constant data are limited and of poor quality (Data Sets C and D), then it is sometimes not possible to determine the stereospecific assignments but the dihedral angles can still be reasonably constrained. When the possibility of local mobility is considered ( $\sigma < 30^\circ$  in Eq. [2] (39)), the results are not very different from those given in Table 4. A summary of the results is given in Table 6.

*Case of conformational averaging.* Similar calculations have been carried out to assess the effects of the quality of the input data on the accuracy of estimated rotamer populations in cases where  $\chi_1$  rotameric averaging is taking place

and the results are shown in Table 5. These calculations use synthetic data related to  $\phi$  and  $\psi$  angles in  $\alpha$ -helices and  $\beta$ -strands combined with a typical distribution of  $\chi_1$  rotamer populations ( $p_{180^\circ} = 0.25$ ,  $p_{-60^\circ} = 0.60$ ,  $p_{60^\circ} = 0.15$ ). In all cases, reasonable values for the populations were predicted even when using the lowest-quality data set (Data Set C), although errors of up to  $\pm 0.2$  would be expected. It was possible to make stereospecific assignments using any of the data sets (A to C). It was found that if low-quality Data Set C is used together with the option of directly fitting the measured and calculated intensities from HNHB experiments, then this gives fractional populations with errors comparable to those obtained by using data sets with higher-quality coupling constant information (such as Data Set A or B).

It is seen that the availability of coupling constant information is always very important. It is also essential to have distance-related data from 2D ROESY or 3D  $^{15}\text{N}$  or  $^{13}\text{C}$  ROESY-HMQC experiments in order to determine ranges of torsion angles, stereospecific assignments, and rotamer populations. A summary of the results obtained by using data sets of different quality is given in Table 6 where it is assumed that such distance-related information is available in all cases.

## APPLICATION TO A PROTEIN

### *Residues Determined by $\phi$ , $\psi$ , and $\chi_1$ Dihedral Angles and Their Stereospecific Assignments*

Residues determined by  $\phi$ ,  $\psi$ , and  $\chi_1$  torsion angles include all amino acids in proteins except for Ala and Gly residues, which will be discussed separately. The initial calculations assume a fixed conformation but subsequently the input data are reexamined under the assumption that there is an averaging of the  $\chi_1$  rotamers. Table 1 indicates the type of

TABLE 6

Results Expected from AngleSearch when Coupling Constant Data of Different Qualities are Available (Assuming a Full Set of ROESY Effects between all Pairs of Atoms (HN, H $\alpha$ , H $\beta$ , H $\beta'$ , and HN $^{i+1}$ ) Except H $\alpha$ -H $\beta$  and H $\alpha$ -H $\beta'$  and is Available)

Quality of measured coupling constants available	Results from AngleSearch
(a) Rough estimates of $^1\text{H}$ - $^1\text{H}$ coupling constants (small, medium, large). No heteronuclear coupling constants.	(a) Stereospecific assignments for more than 50% residues Ranges for calculated torsion angles $\sim \pm 30^\circ$ . Rotamer populations cannot be obtained.
(b) Rough estimates of both $^1\text{H}$ - $^1\text{H}$ and $^{15}\text{N}$ - $^1\text{H}$ coupling constants (small, medium, large).	(b) Stereospecific assignments for most residues; ranges for calculated torsion angles $\sim \pm 20^\circ$ . Rotamer populations can be calculated ( $\pm 0.2$ ).
(c) $^1\text{H}$ - $^1\text{H}$ coupling constants (better than $\pm 2$ Hz). $^{15}\text{N}$ - $^1\text{H}$ coupling constants (better than $\pm 2$ Hz or use of intensities from HNHB experiments).	(c) Stereospecific assignments for most residues; ranges for calculated torsion angles $< \pm 20^\circ$ . Rotamer populations can be calculated ( $\pm 0.1$ ).
(d) $^1\text{H}$ - $^1\text{H}$ coupling constants (better than $\pm 2$ Hz). $^{15}\text{N}$ - $^1\text{H}$ coupling constants, $^{13}\text{C}$ - $^1\text{H}$ coupling constants (better than $\pm 2$ Hz or use of intensities from HNHB and HN(CO)HB experiments).	(d) Stereospecific assignments for most residues; ranges for calculated torsion angles $< \pm 15^\circ$ . Rotamer populations can be calculated (better than $\pm 0.1$ ).

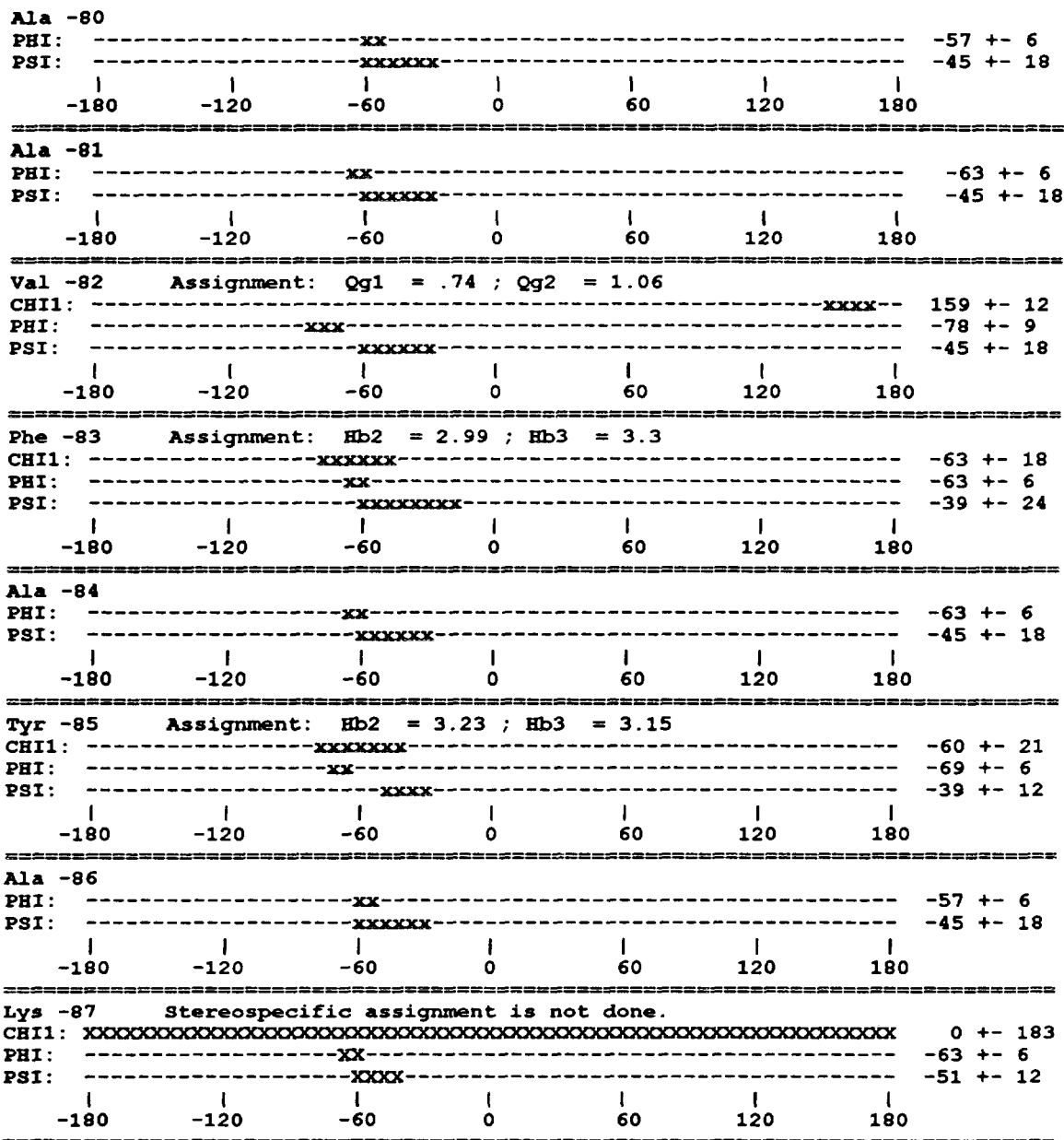


FIG. 2. Typical output from AngleSearch for residues Ala-80-Lys-87 in the DHFR-MTX complex.

measured data required in order to calculate the above conformational information. Starting with an arbitrary assignment for the  $\beta$ -methylene protons in each particular side chain, AngleSearch calculates ranges of the  $\phi$ ,  $\psi$ , and  $\chi_1$  values which are consistent with the input data, assuming a fixed conformation. The calculations are then repeated with the assignments of the  $\beta$ -methylene protons reversed. Usually, where good-quality data are available, only one of the two sets of possible stereospecific assignments gives a range of torsion angles fully consistent with the data. In this case, the method provides a clear-cut stereospecific assignment for the  $\beta$ -methylene protons as well as the  $\phi$ ,  $\psi$ , and  $\chi_1$  tor-

sion-angle constraints. In cases where lower-quality input data are available, both sets of stereospecific assignments may give solutions of allowed torsion angles: for these, the stereospecific assignments cannot be made using AngleSearch alone and the ranges of torsion-angle solutions then embrace all the values predicted by both sets of assignments.

The program has been used to obtain detailed conformational information for complexes formed by binding various antifolate drugs (methotrexate, trimethoprim, and trimetrexate) to *L. casei* DHFR. Figure 2 shows a typical output from AngleSearch in which crosses are used to indicate the allowed torsion angles, so that all the possible combinations

**TABLE 7**  
**Torsion Angles, Stereospecific Assignments, and  $\chi_1$  Rotameric Populations for Representative Stretch of Sequence in the DHFR.MTX Complex**

Residue	Torsion angles					Rotameric populations $\chi_1$			Stereospecific assignment (ppm)
	$\phi$	$\psi$	$\chi_1$	$\chi_2$	$\omega$	$p_{180^\circ}$	$p_{-60^\circ}$	$p_{60^\circ}$	
Glu-93	$-120^\circ \pm 51^\circ$	$168^\circ \pm 21^\circ$	$-51^\circ \pm 24^\circ$	—	$180^\circ$	(2)	(2)	(2)	$H_{\beta^2} = 1.78$ ; $H_{\beta^3} = 2.00$
Leu-94	$-120^\circ \pm 39^\circ$	$114^\circ \pm 51^\circ$	$-60^\circ \pm 33^\circ$	(1)	$180^\circ$	(1)	(1)	(1)	(1)
Val-95	$-117^\circ \pm 24^\circ$	$123^\circ \pm 60^\circ$	$168^\circ \pm 15^\circ$	—	$180^\circ$	(1)	(1)	(1)	(1)
Ile-96	$-120^\circ \pm 33^\circ$	$120^\circ \pm 39^\circ$	$-57^\circ \pm 30^\circ$	$-60^\circ \pm 27^\circ$	$180^\circ$	$0.15 \pm 0.15$	$0.85 \pm 0.15$	$0.0 \pm 0.05$	$H_{\gamma^{11}} = 1.41$ ; $H_{\gamma^{12}} = 0.84$
Ala-97	$-120^\circ \pm 15^\circ$	$-18^\circ \pm 69^\circ$	—	—	$180^\circ$	—	—	—	—
Gly-98	$63^\circ \pm 12^\circ$	$60^\circ \pm 63^\circ$	—	—	$0^\circ$	—	—	—	$H_{\alpha^1} = 4.16$ ; $H_{\alpha^2} = 2.20$ (3)
Gly-99	$-81^\circ \pm 6^\circ$	$-114^\circ \pm 69^\circ$	—	—	$180^\circ$	—	—	—	$H_{\alpha^1} = 3.70$ ; $H_{\alpha^2} = 4.00$ (3)
Ala-100	$-48^\circ \pm 9^\circ$	$-36^\circ \pm 15^\circ$	—	—	$180^\circ$	—	—	—	—
Gln-101	$-69^\circ \pm 12^\circ$	$-42^\circ \pm 15^\circ$	(4)	—	$180^\circ$	(4)	(4)	(4)	Not determined (4)
Ile-102	$-87^\circ \pm 6^\circ$	$-60^\circ \pm 27^\circ$	$-78^\circ \pm 15^\circ$	(2)	$180^\circ$	$0.05 \pm 0.05$	$0.75 \pm 0.15$	$0.20 \pm 0.10$	(2)
Phe-103	$-57^\circ \pm 6^\circ$	$-60^\circ \pm 33^\circ$	$-75^\circ \pm 12^\circ$	—	$180^\circ$	$0.05 \pm 0.05$	$0.75 \pm 0.05$	$0.20 \pm 0.05$	$H_{\beta^2} = 2.68$ ; $H_{\beta^3} = 2.49$
Thr-104	$-57^\circ \pm 6^\circ$	$-54^\circ \pm 27^\circ$	Averaged	—	$180^\circ$	$0.25 \pm 0.10$	$0.20 \pm 0.10$	$0.55 \pm 0.15$	—
Ala-105	$-63^\circ \pm 6^\circ$	$-45^\circ \pm 18^\circ$	—	—	$180^\circ$	—	—	—	—
Phe-106	$-120^\circ \pm 27^\circ$	$36^\circ \pm 33^\circ$	$-66^\circ \pm 27^\circ$	—	$180^\circ$	$0.10 \pm 0.10$	$0.65 \pm 0.10$	$0.25 \pm 0.05$	$H_{\beta^2} = 2.94$ ; $H_{\beta^3} = 3.86$
Lys-107	$-48^\circ \pm 9^\circ$	$-36^\circ \pm 6^\circ$	(1)	—	$180^\circ$	(1)	(1)	(1)	(1)
Asp-108	$-87^\circ \pm 6^\circ$	$-42^\circ \pm 45^\circ$	Averaged	—	$180^\circ$	$0.05 \pm 0.05$	$0.65 \pm 0.05$	$0.30 \pm 0.05$	$H_{\beta^2} = 2.51$ ; $H_{\beta^3} = 2.78$
Asp-109	$-120^\circ \pm 15^\circ$	$27^\circ \pm 24^\circ$	Averaged	—	$180^\circ$	$0.10 \pm 0.10$	$0.65 \pm 0.10$	$0.25 \pm 0.05$	$H_{\beta^2} = 2.64$ ; $H_{\beta^3} = 3.07$
Val-110	$-69^\circ \pm 6^\circ$	$117^\circ \pm 30^\circ$	$78^\circ \pm 15^\circ$	—	$180^\circ$	$0.10 \pm 0.10$	$0.10 \pm 0.10$	$0.80 \pm 0.20$	$H_{\gamma^1} = 0.40$ ; $H_{\gamma^2} = 0.34$
Asp-111	$-111^\circ \pm 12^\circ$	$-27^\circ \pm 12^\circ$	Averaged	—	$180^\circ$	$0.20 \pm 0.10$	$0.45 \pm 0.05$	$0.35 \pm 0.05$	$H_{\beta^2} = 2.70$ ; $H_{\beta^3} = 2.94$
Thr-112	$-120^\circ \pm 21^\circ$	$141^\circ \pm 18^\circ$	$-45^\circ \pm 18^\circ$	—	$180^\circ$	$0.20 \pm 0.20$	$0.75 \pm 0.20$	$0.05 \pm 0.05$	—
Leu-113	$-120^\circ \pm 21^\circ$	$120^\circ \pm 51^\circ$	$-57^\circ \pm 30^\circ$	$-63^\circ \pm 30^\circ$	$180^\circ$	$0.10 \pm 0.10$	$0.90 \pm 0.10$	$0.0 \pm 0.05$	$H_{\beta^2} = 1.85$ ; $H_{\beta^3} = 1.38$ $H_{\beta^1} = -1.00$ ; $H_{\beta^2} = 0.25$ $H_{\beta^1} = 0.91$ ; $H_{\beta^2} = 1.02$
Leu-114	$-120^\circ \pm 27^\circ$	$120^\circ \pm 51^\circ$	$-60^\circ \pm 33^\circ$	$-66^\circ \pm 27^\circ$	$180^\circ$	$0.15 \pm 0.15$	$0.70 \pm 0.15$	$0.15 \pm 0.05$	$H_{\beta^2} = 2.55$ ; $H_{\beta^3} = 1.58$ $H_{\beta^1} = 0.91$ ; $H_{\beta^2} = 1.02$
Val-115	$-120^\circ \pm 9^\circ$	$156^\circ \pm 27^\circ$	(2)	—	$180^\circ$	(2)	(2)	(2)	(2)
Thr-116	$-120^\circ \pm 9^\circ$	$144^\circ \pm 9^\circ$	$-18^\circ \pm 9^\circ$	—	$180^\circ$	(5)	(5)	(5)	—
Arg-117	$-117^\circ \pm 24^\circ$	$114^\circ \pm 45^\circ$	$78^\circ \pm 12^\circ$	—	$180^\circ$	(5)	(5)	(5)	$H_{\beta^2} = 1.68$ ; $H_{\beta^3} = 1.32$
Leu-118	$-87^\circ \pm 6^\circ$	$144^\circ \pm 27^\circ$	$-78^\circ \pm 15^\circ$	$-81^\circ \pm 12^\circ$	$180^\circ$	(5)	(5)	(5)	$H_{\beta^2} = 1.02$ ; $H_{\beta^3} = 1.83$

Note. (1) Not determined: degenerate chemical shifts. (2) Not determined: overlap of signals. (3) Stereospecific assignment made using approach described under Stereospecific Assignment for Gly Residues. (4) Not enough data: weak signals. (5) No solution for averaging model: nonstaggered conformer.

of allowed torsion angles are easily visualized. Table 7 gives the torsion-angle constraints, stereospecific assignments, and  $\chi_1$  rotameric populations determined by the program for a representative stretch of sequence (Glu-93 to Leu-118) in the DHFR complex with methotrexate. This stretch of sequence contains a  $\alpha$ -helix, two  $\beta$ -strands, and some loop regions (46, 50). Its residues provide examples of most of the conformational situations observed in proteins. Examination of the data indicates that for many of the residues the  $\phi$ ,  $\psi$ , and  $\chi_1$  torsion angles and stereospecific assignments can be determined directly (Glu-93, Phe-103, Phe-106, Asp-109, Val-110, Leu-113, Leu-114, Val-115, Thr-116, Asn-117, and Leu-118).

**Determination of conformations in fragments where there is only a single  $\beta$ -proton.** For residues such as threonine, valine, and isoleucine, there is only one  $\beta$ -proton and thus there is less three-bond proton coupling information available than for other residues. There is also less distance information

between  $\alpha$ - and  $\beta$ -protons but this is compensated for, to some extent, by the distance information available between  $\alpha$ - and  $\gamma$ -methyl protons. This is particularly true for Val residues where there are two  $\gamma$ -CH<sub>3</sub> groups. By treating each of the  $\gamma$ -CH<sub>3</sub> groups as a pseudo-atom and carrying out calculations for the two sets of assignments, AngleSearch can determine the stereospecific assignments of the CH<sub>3</sub> groups and the  $\phi$ ,  $\psi$ , and  $\chi_1$  torsion angles. For threonine and isoleucine, there are no available ratios of parameters to pairs of methylene or methyl protons but this is not so important because there is no longer the need to assign the stereospecificity of the single  $\beta$ -proton for these residues. The program is able to cope with this situation and again gives good  $\phi$ ,  $\psi$ , and  $\chi_1$  torsion-angle information (see Table 7 which includes results for Val-95, Ile-96, Ile-102, Thr-104, Val-110, Thr-112, Val-115, and Thr-116).

**Detection and determination of mixtures of conformations where there is conformational averaging.** One of the most

important options in the AngleSearch program is its ability to analyze averaged data resulting from rotational isomers undergoing fast exchange. In this case, the program fits the observed data to calculated mixtures of rotamers as described earlier. If input data of sufficient quality are available, one can obtain ranges of  $\phi$  and  $\psi$  angles,  $\chi_1$  rotamer populations, and stereospecific assignments which fit the observed data. Such rotameric averaging has been recognized in several previous studies of proteins and the term "disordered" has been applied to describe such residues (19). The program provides a very efficient procedure for locating which residues fall into this category and for interpreting the observed data in terms of mixtures of the interconverting rotamers. Starting with an arbitrary assignment for the  $\beta$ -CH<sub>2</sub> protons, the program calculates  $\phi$  and  $\psi$  angles and  $\chi_1$  rotamer populations consistent with the input data. The calculations are then repeated with the  $\beta$ -CH<sub>2</sub> assignments reversed. In most cases where good-quality data are available, only one set of stereospecific assignments leads to a good solution. For most residues in the DHFR-MTX complex, the side chain is found to be predominantly in a single  $\chi_1$  conformation; however, for some residues, the data can only be satisfied by a mixture of rotamers. One can often detect when rotational averaging is taking place by observing similar large values for the apparent coupling constants between  $\alpha$ -CH and both the  $\beta$ -CH<sub>2</sub> protons or between <sup>15</sup>N (NH) and both the  $\beta$ -CH<sub>2</sub> protons.

For larger proteins where accurate values of coupling constants are not available, it is necessary to rely on coupling constant-related intensities of cross peaks (in experiments such as HNHB and HN(CO)HB) as discussed earlier. In this case, each  $\chi_1$  rotamer can be characterized by a ratio of intensities related to the appropriate three-bond coupling constants: because the intensities can be measured with relatively high precision, this improves the precision of the calculated rotamer populations. In the DHFR-methotrexate complex, several examples of residues existing as mixtures of  $\chi_1$  rotamers were found and these are indicated in Table 7 (for example, Thr-104, Asp-108, Asp-109, and Asp-111).

#### *Residues Determined by $\phi$ and $\psi$ Only*

Gly and Ala residues are fully defined by the variable backbone torsion angles  $\phi$  and  $\psi$  and these can be determined by using the appropriate input data (see Table 1) with the AngleSearch program. For Ala residues, the AngleSearch program can fully define the  $\phi$  and  $\psi$  backbone angles. There is usually sufficient NOE data involving the Ala  $\alpha$ -CH,  $\beta$ -CH<sub>3</sub>, and NH protons to provide well-defined angles.

*Stereospecific assignments for Gly residues.* A valuable function of the AngleSearch program is the assistance it provides in making stereospecific assignments of the  $\alpha$ -CH<sub>2</sub> protons of glycine residues. This is achieved by combining predictions from AngleSearch with torsion-angle results ob-

tained from structures of fairly low quality calculated using restrained molecular dynamics.

We have been able to make several such assignments for glycine residues in complexes of dihydrofolate reductase. Starting with an arbitrary set of assignments for a particular glycine  $\alpha$ -CH<sub>2</sub> group, the ranges for the  $\phi$  and  $\psi$  angles consistent with the input data were calculated; a typical output is shown in Fig. 3a for Gly-11 of the DHFR-methotrexate complex. The calculations were repeated with the assignments for the  $\alpha$ -methylene protons reversed and a new set of allowed range of  $\phi$  and  $\psi$  calculated (given in Fig. 3a). Finally, ranges of  $\phi$  and  $\psi$  were also obtained by using restrained molecular dynamic calculations to determine the solution structure of the DHFR-methotrexate complex where the glycine methylene protons are included in the calculation as pseudo-atoms. The ranges of  $\phi$  and  $\psi$  found by the program are compared with the ranges resulting from the restrained molecular dynamics calculations. In favorable cases, the ranges overlap with only one of the two possible sets of stereospecific assignments. The ranges of  $\phi$  and  $\psi$  angles which are found in 17 calculated structures are shown for Gly-11 in Fig. 3b. It is seen that only one set of stereospecific assignments for the methylene protons (given in Fig. 3b) gives torsion angles in close agreement with the ranges obtained from the structure calculations. Thus, in this case, there is an unequivocal stereospecific assignment for the two  $\alpha$ -protons: such assignments could be made for six of the nine Gly residues in the DHFR-MTX complex.

The X-Gly peptide bond can exist in both cis and trans configurations and the option for investigating these possibilities is included in the program.

#### *Residues Determined by $\phi$ , $\psi$ , $\chi_1$ , and $\chi_2$*

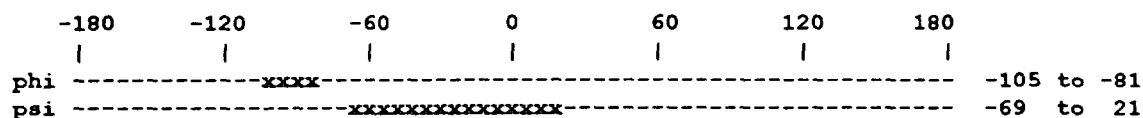
For some residues, such as leucine and isoleucine, it is possible to obtain further side-chain conformational information by determining both  $\chi_1$  and  $\chi_2$ . Table 2 indicates the wide variety of coupling constant and interproton distances which are related to the  $\chi_2$  dihedral angle for these residues. For rotameric averaging, the three staggered conformations about the C $\beta$ -C $\gamma$  bond for Leu and Ile residues were considered. For these residues, AngleSearch was first used to determine  $\phi$ ,  $\psi$ , and  $\chi_1$  in the manner described earlier. In the case of leucine, the  $\beta$ -CH<sub>2</sub> stereospecific assignments were also made at this stage. The program was then used to examine the fragment described by  $\phi$ ,  $\chi_1$ , and  $\chi_2$ , using input data of the type indicated in Table 2. In the case of leucine, the calculation is first carried out with an arbitrary assignment of the  $\delta$ -CH<sub>3</sub> protons and then repeated using the reverse assignment. If the  $\beta$ -CH<sub>2</sub> protons have been stereospecifically assigned, this procedure results in only one solution of  $\phi$ ,  $\chi_1$ , and  $\chi_2$ , thus giving the stereospecific assignments for the  $\delta$ -CH<sub>3</sub> protons and the torsion angles. Essentially the same procedure was followed for isoleucine by carrying out the calculations for the two possible sets of ste-

## Results of calculation for residue Gly-11 :

## 1. Initial set of prochiral atoms.

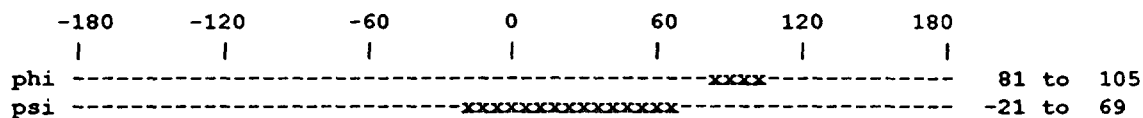
Number of points= 0000044

(a)



## 2. Atoms Ha1 and Ha2 were swapped.

Number of points= 0000044



## Families of angles from MD calculations for residue Gly-11:

(b)

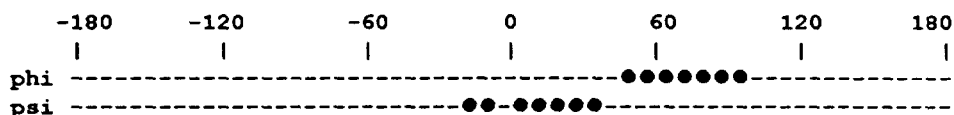


FIG. 3. Determination of stereospecific assignment of the  $\alpha$ -methylene protons for Gly 11 in the DHFR-MTX complex: (a) Results from AngleSearch and (b) results from 17 structures calculated by simulated annealing and representing Gly methylene protons as pseudo-atoms.

reospecific assignments for the  $\gamma$ -CH<sub>2</sub> protons. Based on such considerations,  $\chi_1$  and  $\chi_2$  torsion angles were determined for several residues in the DHFR-methotrexate complex (see Ile-96, Leu-113, Leu-114, and Leu-118 in Table 7).

A full discussion of the stereospecific assignments, torsion-angle constraints, and rotamer population obtained for all the residues in the complexes of DHFR with methotrexate and other ligands will be given elsewhere.

## ACKNOWLEDGMENTS

The NMR measurements were made using the facilities at the MRC Biomedical NMR Centre, National Institute for Medical Research, Mill Hill. V. I. Polshakov acknowledges the award of a Wellcome Trust Fellowship. We thank A. Gargaro for assistance with MD calculations, C. J. Bauer, G. Martorell, and A. N. Lane for helpful discussions, G. Ostler and J. E. McCormick for expert technical assistance, and L. Dunphy for processing the manuscript.

## REFERENCES

1. K. Wüthrich, "NMR of Proteins and Nucleic Acids," Wiley, New York, 1987.
2. E. R. P. Zuiderweg, R. Boelens, and R. Kaptein, *Biopolymers* **24**, 601 (1985).
3. S. G. Hyberts, W. Märki, and G. Wagner, *Eur. J. Biochem.* **164**, 625 (1987).
4. G. M. Clore and A. M. Gronenborn, *CRC Crit. Rev. Biochem. Mol. Biol.* **24**, 479 (1989).
5. P. C. Driscoll, A. M. Gronenborn, and G. M. Clore, *FEBS Lett.* **243**, 223 (1989).
6. A. Arseniev, P. Schultze, E. Wörgötter, W. Braun, G. Wagner, M. Vasak, J. H. R. Kägi, and K. Wüthrich, *J. Mol. Biol.* **201**, 637 (1988).
7. P. L. Weber, R. Morrison, and D. Hare, *J. Mol. Biol.* **204**, 483 (1988).
8. G. Wagner, *Prog. NMR Spectrosc.* **22**, 101 (1990).
9. P. E. Hansen, J. Feeney, and G. C. K. Roberts, *J. Magn. Reson.* **17**, 249 (1975).
10. H. Kessler, C. Griesinger, and K. Wagner, *J. Am. Chem. Soc.* **109**, 6927 (1987).
11. G. Wagner, W. Braun, T. F. Havel, T. Schaumann, N. Go, and K. Wüthrich, *J. Mol. Biol.* **196**, 611 (1987).
12. P. Güntert, W. Braun, M. Billeter, and K. Wüthrich, *J. Am. Chem. Soc.* **111**, 3997 (1989).
13. Ž. Džakula, A. S. Edison, W. M. Westler, and J. L. Markley, *J. Am. Chem. Soc.* **114**, 6200 (1992).
14. M. Nilges, G. M., Clore, and A. M. Gronenborn, *Biopolymers* **29**, 813 (1990).
15. P. Güntert, W. Braun, and K. Wüthrich, *J. Mol. Biol.* **217**, 517 (1991).
16. A. Bax and R. Freeman, *J. Magn. Reson.* **44**, 542 (1981).
17. C. Griesinger, O. W. Sørensen, and R. R. Ernst, *J. Am. Chem. Soc.* **107**, 6394 (1985).
18. L. Mueller, *J. Magn. Reson.* **72**, 191 (1987).
19. G. M. Clore, A. Bax, and A. M. Gronenborn, *J. Biomol. NMR* **1**, 13 (1991).

20. G. W. Vuister and A. Bax, *J. Am. Chem. Soc.* **115**, 7772 (1993).
21. S. J. Archer, M. Ikura, D. A. Torchia, and A. Bax, *J. Magn. Reson.* **95**, 636 (1991).
22. S. Grzesiek, M. Ikura, G. M. Clore, A. M. Gronenborn, and A. Bax, *J. Magn. Reson.* **96**, 215 (1992).
23. A. A. Bothner-By, R. L. Stephens, J. Lee, C. D. Warren, and R. W. Jeanloz, *J. Am. Chem. Soc.* **106**, 811 (1984).
24. G. M. Clore, A. Bax, P. T. Wingfield, and A. M. Gronenborn, *Biochemistry* **29**, 5671 (1990).
25. M. Rance, O. W. Sørensen, G. Bodenhausen, G. Wagner, R. R. Ernst, and K. Wüthrich, *Biochem. Biophys. Res. Commun.* **117**, 479 (1983).
26. D. Marion, P. C. Driscoll, L. E. Kay, P. T. Wingfield, A. Bax, A. M. Gronenborn, and G. M. Clore, *Biochemistry* **28**, 6150 (1989).
27. A. Bax, S. W. Sparks, and D. A. Torchia, *J. Am. Chem. Soc.* **110**, 7926 (1988).
28. R. Weisemann, H. Rüterjans, H. Schwalbe, J. Schleucher, W. Bermel, and C. Griesinger, *J. Biomol. NMR* **4**, 231 (1994).
29. G. W. Vuister and A. Bax, *J. Magn. Reson. B* **102**, 228 (1993).
30. U. Eggenber, Y. Karini-Nejad, H. Thüning, H. Rüterjans, and C. Griesinger, *J. Biomol. NMR* **2**, 583 (1992).
31. K. L. Constantine, M. S. Friedrichs, and L. Mueller, *J. Magn. Reson. B* **104**, 62 (1994).
32. G. W. Vuister, T. Yamazaki, D. A. Torchia, and A. Bax, *J. Biomol. NMR* **3**, 297 (1993).
33. A. Bax, D. Max, and D. Zax, *J. Am. Chem. Soc.* **114**, 6923 (1992).
34. F. Fogolari, G. Esposito, S. Cauci, and P. Viglino, *J. Magn. Reson. A* **102**, 49 (1993).
35. V. F. Bystrov, *Prog. NMR Spectrosc.* **10**, 71 (1976).
36. A. DeMarco, M. Llinás, and K. Wüthrich, *Biopolymers* **17**, 617 (1978).
37. A. DeMarco, M. Llinás, and K. Wüthrich, *Biopolymers* **17**, 2727 (1978).
38. A. J. Fischman, O. H. Live, H. R. Wyssbrod, W. E. Agosta, and D. Cowburn, *J. Am. Chem. Soc.* **102**, 2533 (1980).
39. Y. Karimi-Nejad, J. M. Schmidt, and H. Rüterjans, *Biochemistry* **33**, 5481 (1994).
40. C. Griesinger, O. W. Sørensen, and R. R. Ernst, *J. Magn. Reson.* **75**, 474 (1987).
41. G. W. Vuister, F. Delaglio, and A. Bax, *J. Biomol. NMR* **3**, 67 (1993).
42. G. W. Vuister and A. Bax, *J. Biomol. NMR* **2**, 401 (1992).
43. G. W. Vuister and A. Bax, *J. Biomol. NMR* **4**, 193 (1994).
44. C. J. Bauer, T. A. Frenkiel, and A. N. Lane, *J. Magn. Reson.* **87**, 144 (1990).
45. J. Andrews, G. M. Clore, R. W. Davies, A. M. Gronenborn, B. Gronenborn, D. Kalderon, P. C. Papadopoulos, S. Schafer, P. F. G. Sims, and R. Stancombe, *Gene* **35**, 217 (1985).
46. M. D. Carr, B. Birdsall, T. A. Frenkiel, C. J. Bauer, J. Jimenez-Barbero, V. I. Polshakov, J. E. McCormick, G. C. K. Roberts, and J. Feeney, *Biochemistry* **30**, 6330 (1991).
47. A. Soteriou, M. D. Carr, T. A. Frenkiel, J. E. McCormick, C. J. Bauer, D. Šali, B. Birdsall, and J. Feeney, *J. Biomol. NMR* **3**, 535 (1993).
48. J. G. Dann, G. Ostler, R. A. Bjur, R. W. King, P. Scudder, P. C. Turner, G. C. K. Roberts, A. S. V. Burgen, and N. G. L. Harding, *Biochem. J.* **157**, 559 (1976).
49. W. H. Press, B. P. Flannery, S. A. Teukolsky, and W. T. Vetterling, "Numerical Recipes in C. The Art of Scientific Computing," Cambridge Univ. Press, New York, 1988.
50. J. T. Bolin, D. J. Filman, D. A. Matthews, R. C. Hamlin, and J. Kraut, *J. Biol. Chem.*, **257**, 13,650 (1982).